Detectors in Particle Physics

1. Interactions of particles and radiation with matter (brief recap)
2. Tracking detectors, vertexing and magnetic spectrometry
3. Calorimeters
4. Particle identification
5. Detector systems

1. Interactions of particle and radiation w/ matter

Energy loss of heavy charged particles: (m > m_e)

Energy loss of particles from **ionization** of matter atoms through collisions with shell electrons.

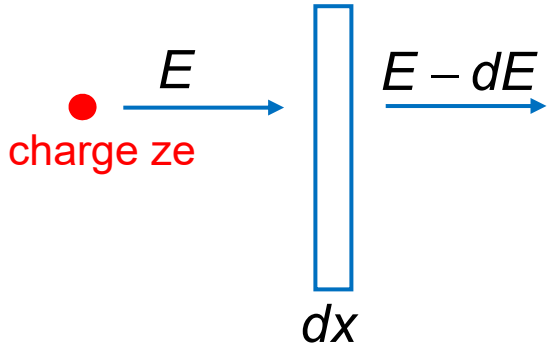

Average specific energy loss dE/dx described by Bethe-Bloch formula

$$\langle \frac{dE}{dx} \rangle_{\text{ion}} = -\underbrace{\left(\rho N_A \frac{Z}{A}\right)}_{n_e} 4\pi r_e^2 m_e c^2 z^2 \cdot \frac{1}{\beta^2} \cdot \left(\ln \frac{2m_e c^2 \gamma^2 \beta^2}{I} - \beta^2\right)$$

ρ = density, n_e= e^- density
N_A = Avogadro number
Z, A = charge number and molar mass
r_e = class. electron radius
I = effective ionization energy

z = charge of the projectile
β = velocity of the projectile

$$r_e = \frac{e^2}{4\pi m_e c^2}$$

To reduce the material dependence one often divides the specific energy loss by the material density ρ

$$\left\langle \frac{dE}{dx} \right\rangle \rightarrow \left\langle \frac{1}{\rho}\frac{dE}{dx} \right\rangle = \left\langle \frac{dE}{dx'} \right\rangle$$

(this is often hidden by redefining the $\rho x \rightarrow x'$

$$\left\langle \frac{dE}{dx'} \right\rangle = \frac{1}{\rho}\left\langle \frac{dE}{dx} \right\rangle = -\underbrace{\left(N_A 4\pi r_e^2 m_e c^2\right)}_{K} z^2 \frac{Z}{A} \cdot \frac{1}{\beta^2} \cdot \left(\ln \frac{2m_e c^2 \gamma^2 \beta^2}{I} - \beta^2 \right)$$

$$K/A = 0.307\,\mathrm{MeV\,g^{-1}\,cm^2} \text{ mit } A = 1\,\mathrm{g \cdot Mol^{-1}}$$ (molar mass)

(K = 0.307 MeV cm^2 Mol^{-1})

w/ Z/A≈ 0.5 for most materials: K Z/A ≈ 0.150 MeV g^{-1}cm^2

Energy loss through ionization.

$$-\frac{1}{\rho}\frac{dE}{dx}$$

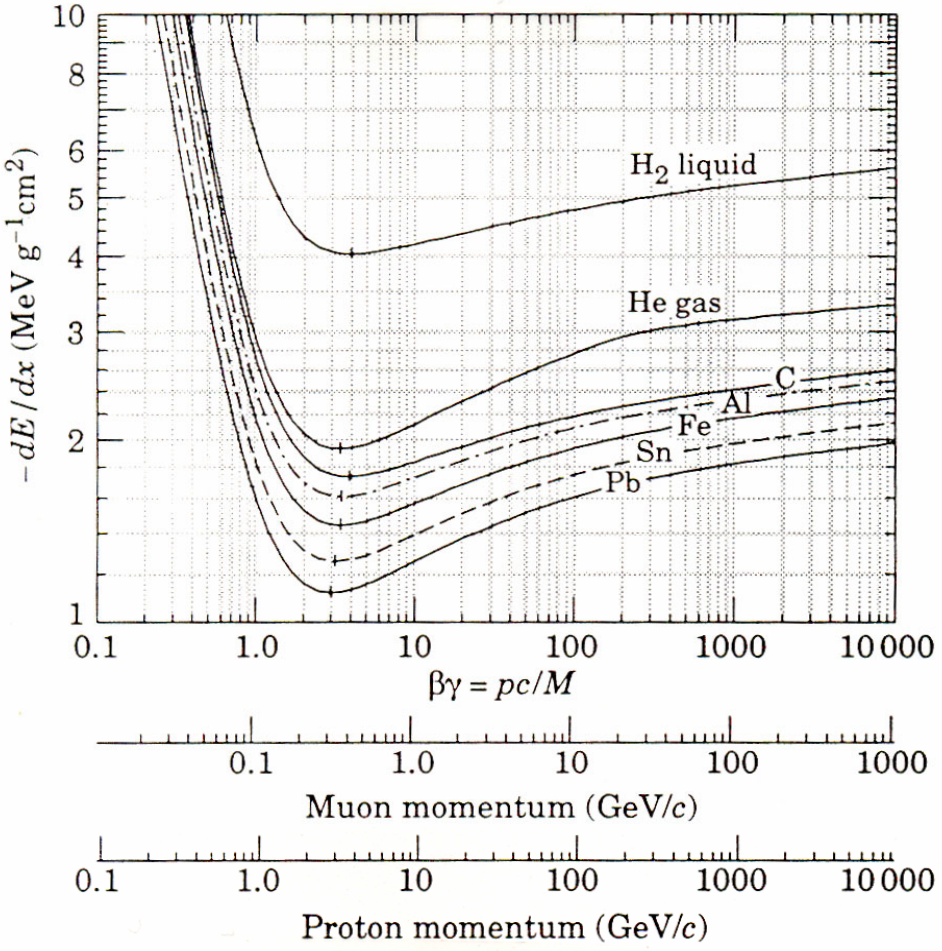

Plot from PDG

difference: Z/A

- ~$1/\beta^2$ for small $\beta\gamma$
- Minimum at $\beta\gamma$ = 3…4 w/ dE/dx =1…2 MeV g^{-1} cm^2 (multiply with ρ to get dE/dx): if one ignores Bremsstrahlung (for muons up to $\beta\gamma$ = O(1000) i.e. 100 GeV ok) particles are quasi "minimal ionizing" also above $\beta\gamma$ of 3.
- For small $\beta\gamma$, dE/dx can be used for particle ID (see below)

Multiple scattering:

Multiple collisions of the projectile with the atoms of the material (stochastic process) leads to a deflection of the particle (and a widening of a beam)

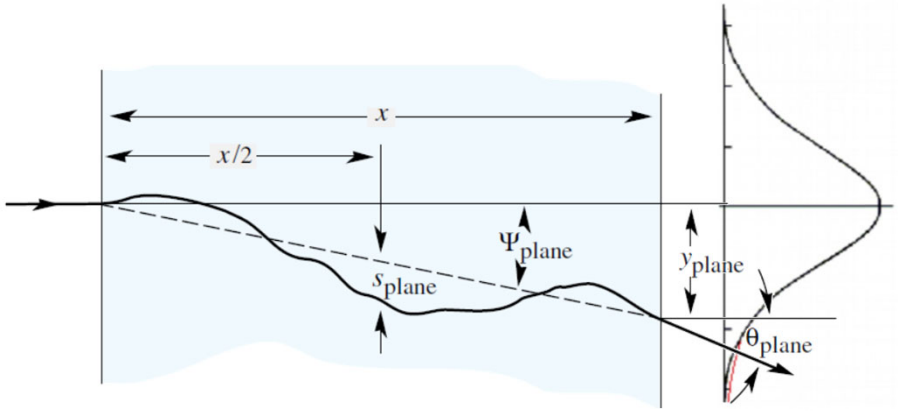

For small angles the deflection probability follows a Gaussian distribution, at least for the central 98%.

$$\frac{1}{\sqrt{2\pi}\,\theta_0}\,\exp\left(-\frac{\theta_{\text{plane}}^2}{2\theta_0^2}\right)$$

For the widths of the Gaussian -depending on whether one measures the deflection in a plane or in 3D - one obtains:

$$\theta_0 = \theta_{\text{plane}}^{\text{rms}} = \frac{1}{\sqrt{2}}\,\theta_{\text{space}}^{\text{rms}}$$

One finds that the width parameter θ_0 depends on the path x through the material in units of the radiation length X_0 and on the particle's momentum. It is significantly less for high momentum particles.

$$\theta_0 = \frac{13.6\ \text{MeV}}{\beta c p}\, z \sqrt{\frac{x}{X_0}}$$

~(√x result form quadratic error propagation)

Cherenkov-radiation: (→ leads to negligible energy loss of the particle)

When a particle traverses a medium with a velocity β (particle velocity β close to c for highly relativistic particles) which is larger than the speed of light within that medium, the particle emits Cherenkov radiation (threshold $\beta > 1/n$).

Cherenkov radiation is emitted on a cone with an opening angle θ_c

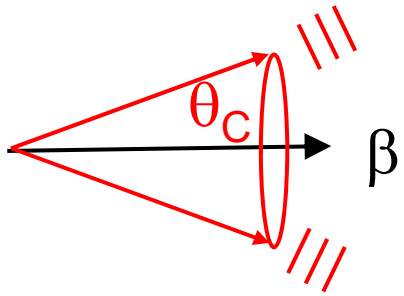

$$\cos\theta_C = \frac{1}{\beta n} = \frac{v_{light,medium}}{v_{particle}}$$

Emitted photons are ranging from **visible blue spectrum to ultraviolet** and The number of photons per unit length of the radiator and per wave-length unit is:

$$\frac{d^2N_\gamma}{dxd\lambda} = \frac{2\pi\alpha z^2}{\lambda^2}\left(1 - \frac{1}{\beta^2 n(\lambda)^2}\right)$$

z is the charge of the particle.

Typical ~1 photon /cm in gas at atmospheric pressure w/ [300,600] nm (300 in water).

To detect photons, medium must be transparent: gases (→ Ring-Cherenkov counter) or water (e.g. large water Cherenkov detectors used for neutrino detection).

Energy loss of electrons (positrons)

For light electrons there are two competing mechanism:

- **Energy loss through ionization** essentially a la **Bethe-Bloch**: **but** max. momentum transfer much larger: $\Delta E = 1/2\ E_{kin}$. Additionally there is the problem that projectile and shell electrons are undistinguishable particles. (Leads to small difference between electrons and positrons).
- **Energy loss through Bremsstrahlung**

$$\langle \frac{dE}{dx} \rangle = \langle \frac{dE}{dx} \rangle_{\text{ion}} + \langle \frac{dE}{dx} \rangle_{\text{Brems}}$$

For high-energy electrons the energy loss by Bremsstrahlung is by far dominating. Only for very low-energy electrons the energy loss by ionization takes over.

Critical energy E_c:

$$\langle \frac{dE}{dx} \rangle_{\text{ion}} \Big|_{E_c} = \langle \frac{dE}{dx} \rangle_{\text{Brems}} \Big|_{E_c}$$

One finds empirically for solid materials: $E_c \approx 610\,\text{MeV}/(Z + 1.2)$

Remark: for lead (Z=82), bremsstrahlung dominates above ~10 MeV

Bremsstrahlung:

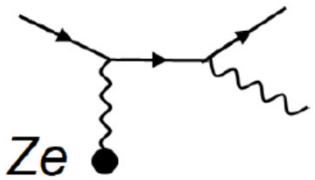

(in presence of a charged nucleus)

Typical length scale for Bremsstrahlung:

Radiation length X_0:

$$\frac{1}{X_0} = \rho N_A \frac{Z^2}{A} \cdot 4\alpha \cdot r_e^2 \cdot \ln\left(\frac{183}{Z^{1/3}}\right)$$

(strong Z dependence)

Energy loss after X_0: $$\langle \frac{dE}{dx} \rangle_{\text{Brems}} = -\frac{1}{X_0} E(x)$$

Energy as function of x: $$E(x) = E_0 e^{-\frac{x}{X_0}}$$

Energy loss of photons

Photons interact in different ways with matter. Most relevant mechanisms:

- Photo-electric effect for low energy photons
- Compton effect for photon energies between 10 keV and MeV
- Pair production for $E_\gamma > 1.02$ MeV ($2m_e$)

Cross section for photons

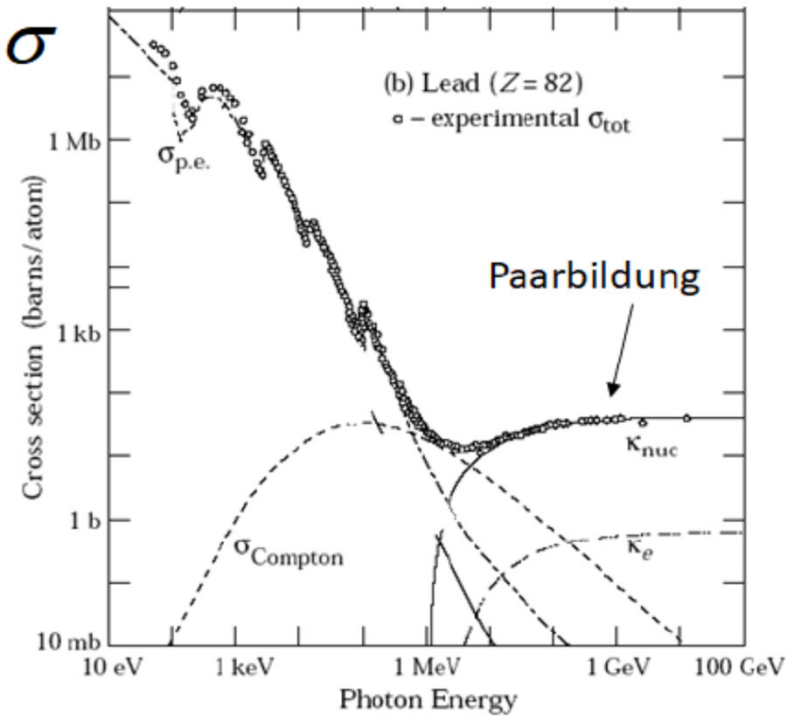

Pair production:

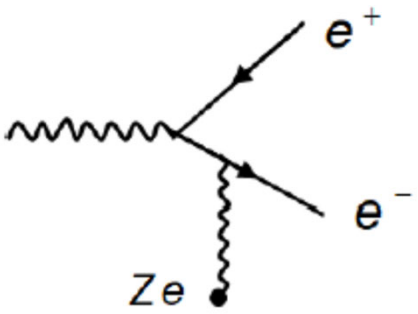

The typical length scale for pair production in matter is again the radiation length X_0.
(both processes w/ similar Feynman diagrams).

An exact calculation however results into
9/7 X_0 - slightly larger than for bremsstrahlung

Pair production cross section for photon energies above 1 GeV is (largely) constant:

$$\sigma_{\text{Paar}} = \frac{7}{9} \cdot \underbrace{\frac{A}{\rho N_A}}_{1/n} \cdot \frac{1}{X_0}$$

Target atom density

Electromagnetic shower: Combination of pair prod. & bremsstrahlung

Simple shower model for high-energy photons/electrons.
Electrons/photons make bremsstrahlung / pair production after ~1X_0

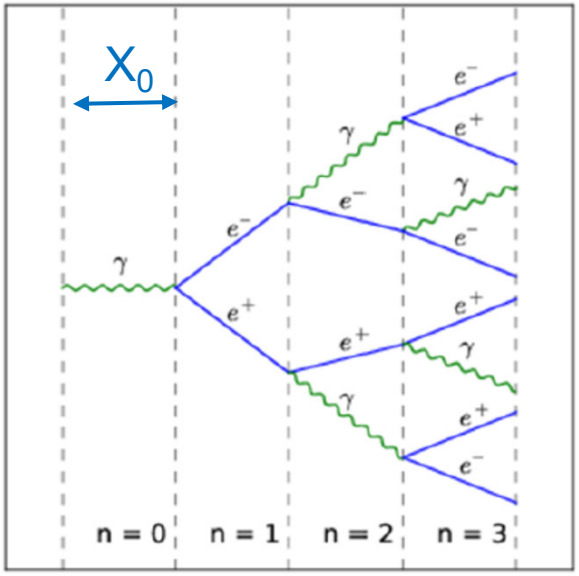

In every step the number of shower particles is doubled: $N(t) = 2^t$

The average energy of the shower particles is E/N – the shower stops when the particle energy has reached the critical energy E_C in the material:

Max. shower depth: $t_{max} = \frac{\ln(E / E_c)}{\ln 2}$

With increasing energy E of the detected particle the calorimeter depth should increase with $\sim \ln(E / E_c)$

$$E / 2^{t_{max}} = E_c$$
$$\rightarrow \ln(E / E_c) = t_{max} \ln 2$$

Hadronic shower

High-energy hadrons (E>>1 GeV) interact with the nuclei and the nucleons of the matter and produce a shower of secondary particles.

$$n, \ , p \, , \pi^{\pm} \, , K^{\pm} \, , K^{0} + A \longrightarrow$$ Shower of secondary particles

Details of the shower are more difficult compared to electromagnetic showers:

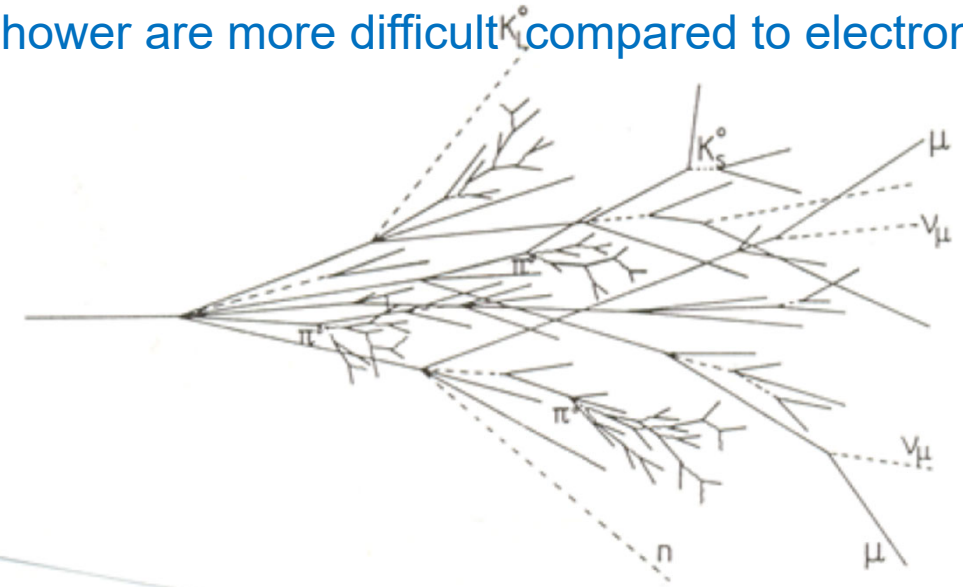

Characteristic interaction length (λ_{int}) for hadrons passing matter is given by:

$$\lambda_{\text{int}} = \frac{1}{n \cdot \sigma_{\text{int}}} = \frac{A}{\rho N_A} \cdot \frac{1}{\sigma_{\text{int}}}$$

Where one finds empirically $\sigma_{\text{int}} \approx 35\,\text{mb}\, A^{0.7}$

Element	λ_{int}
Fe	16.8 cm
Pb	17.6 cm
C	39 cm

2. Tracking, vertexing and magnetic spectrometry

Reconstruct track of charged particle in an magnetic field → use the track curvature to estimate the momentum → reconstruct decay vertices.

Historical example: **Bubble chamber** (by D. Glaser in 1952, Nobel prize in 1960)

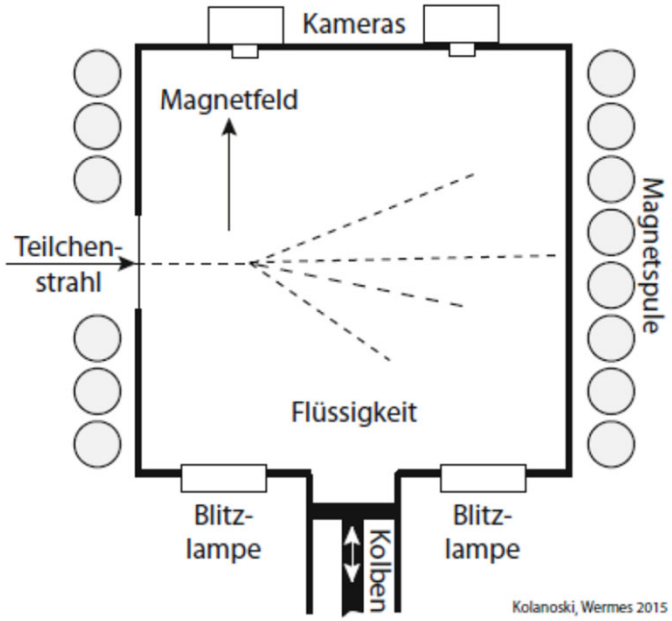

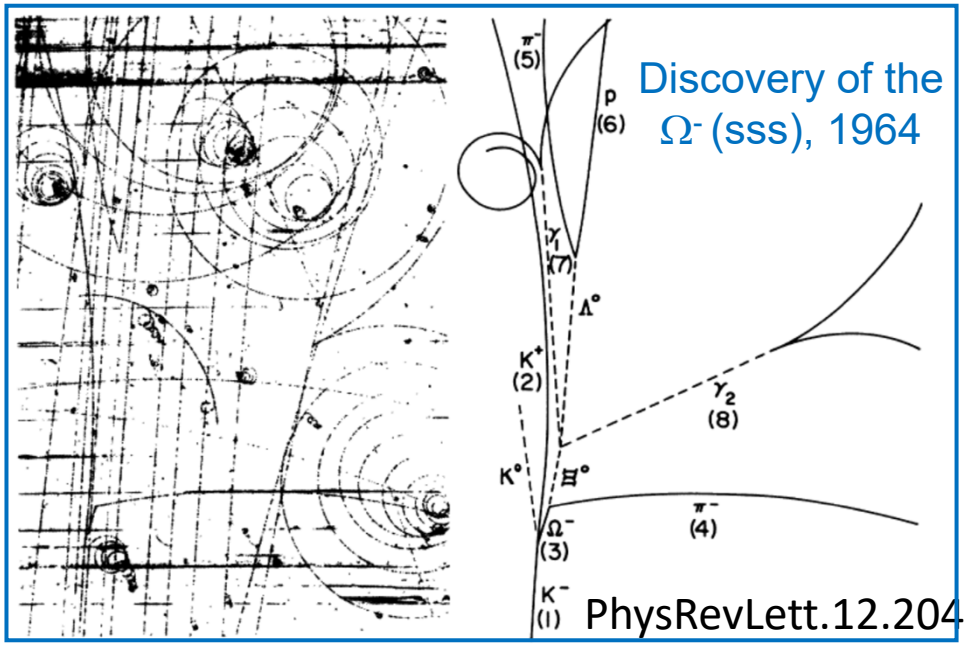

vessel filled with a super-heated transparent liquid (often H_2).

Reconstruction of tracks, decay vertices, momenta.
Disadvantage: photos w/ subsequent digitizations, heavy piston to arm the detector → slow acquisition rate

Multi-wire proportional chambers (MWPCs)

Georges Charpak (1968), Nobel prize in 1992.

Wire chambers have revolutionized **charged particle tracking**:
fully electronic event recording, high data acquisition rates (up to 40 MHz),
excellent position resolution when operated as drift chambers.

Detection principle:

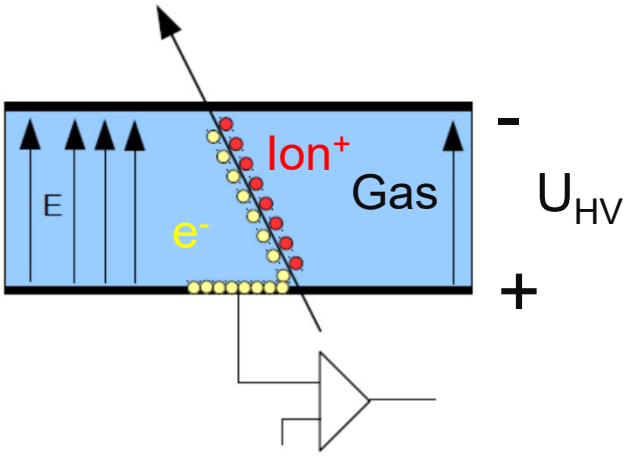

Charge particle ionizes the gas.
Electrons drift towards the anode.
In wire chambers, the anodes are realized by thin wires → amplification due to strong field.
Electronic processing of signals

Thin anode wires – gas amplification

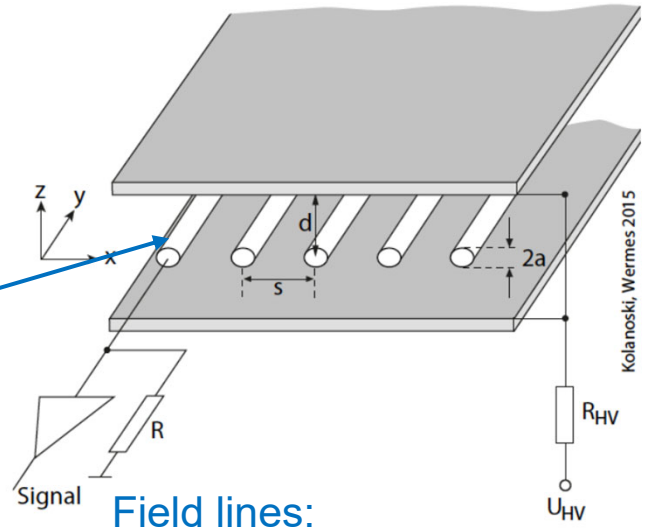

Field lines:
→ electrons guided to anodes

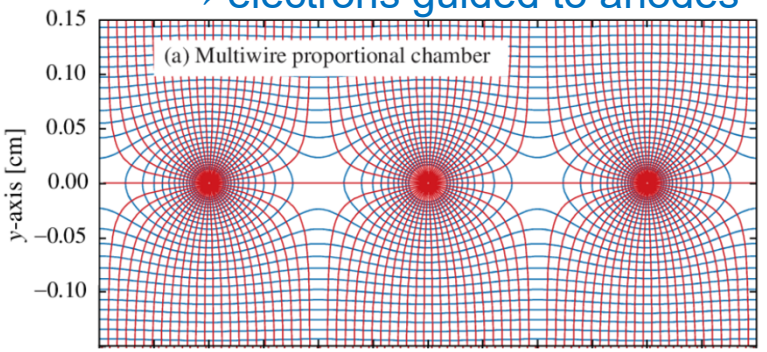

Gas amplification:

Simplest configuration: Wire inside tube:

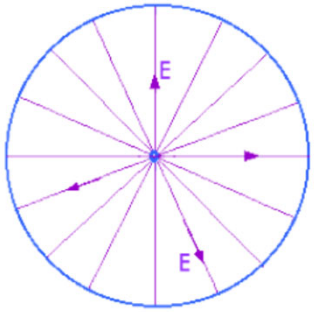

$$E(r) = \frac{U}{r \ln \frac{b}{a}}$$

b = radius of tube
a = radius of wire

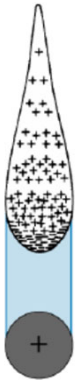

Strong electrical field near the wire leads to acceleration of primary electrons and to further ionization → avalanche: gas amplification. Typ. gain ~10^5

Drift-chambers:

http://ikpe1101.ikp.kfa-juelich.de/

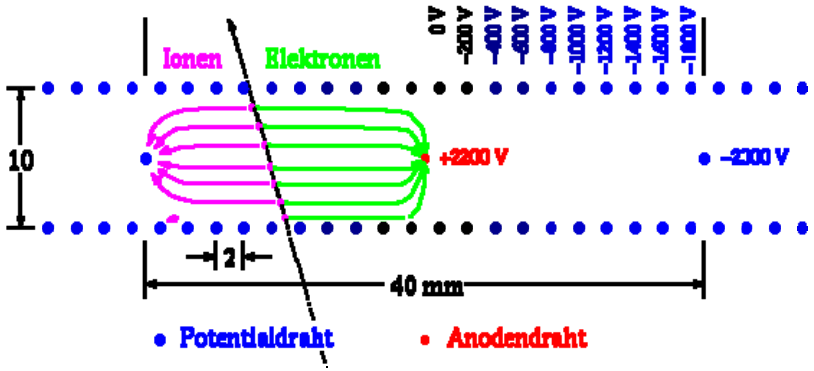

Drift chamber principle was established first in 1970 in Heidelberg (by A. H. Walenta & J. Heintze).

Using special wire configurations one can construct “drift cells” with very homogenous drift paths → one can use the drift time to reconstruct the particle trajectory.

Instead of building drift cells from complicated wire configurations simple tubes with an anode wire can be used:

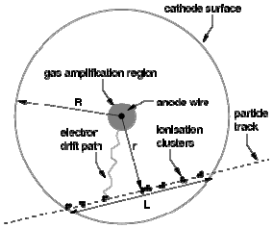

Example 1: JADE Jet-Chamber (1976-1979)

Inner Radius: 20cm
Outer Radius: 80cm
Length: 2.4m

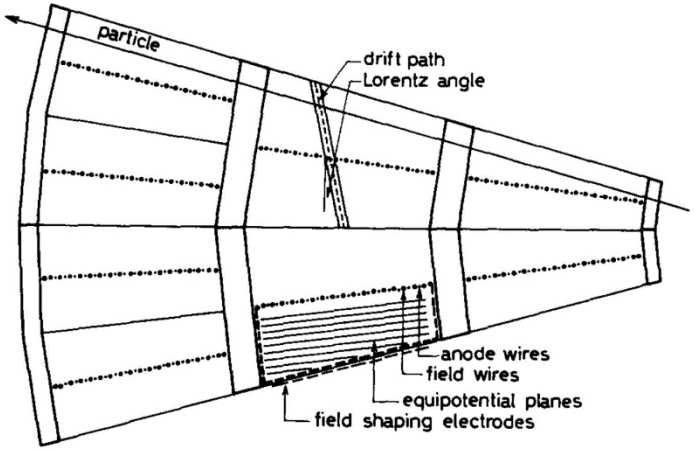

Spatial resolution rφ: 170 μm

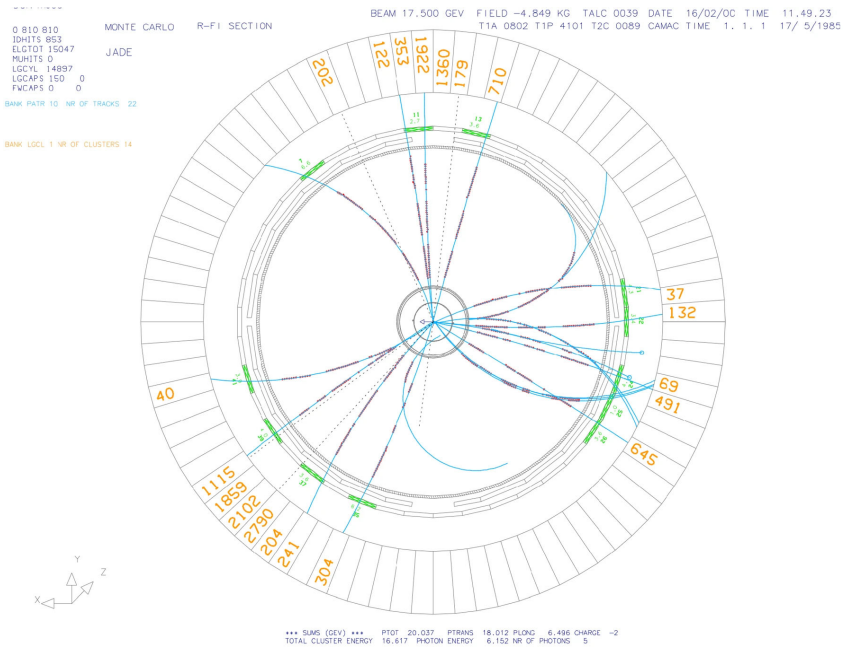

J. Heintze et al.
https://doi.org/10.1016/0029-554X(82)90658-9

Example 2: LHCb Outer Tracker (2001-2008)

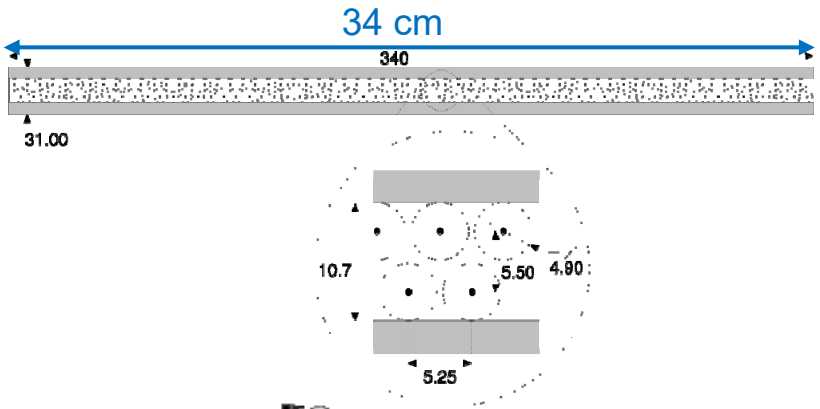

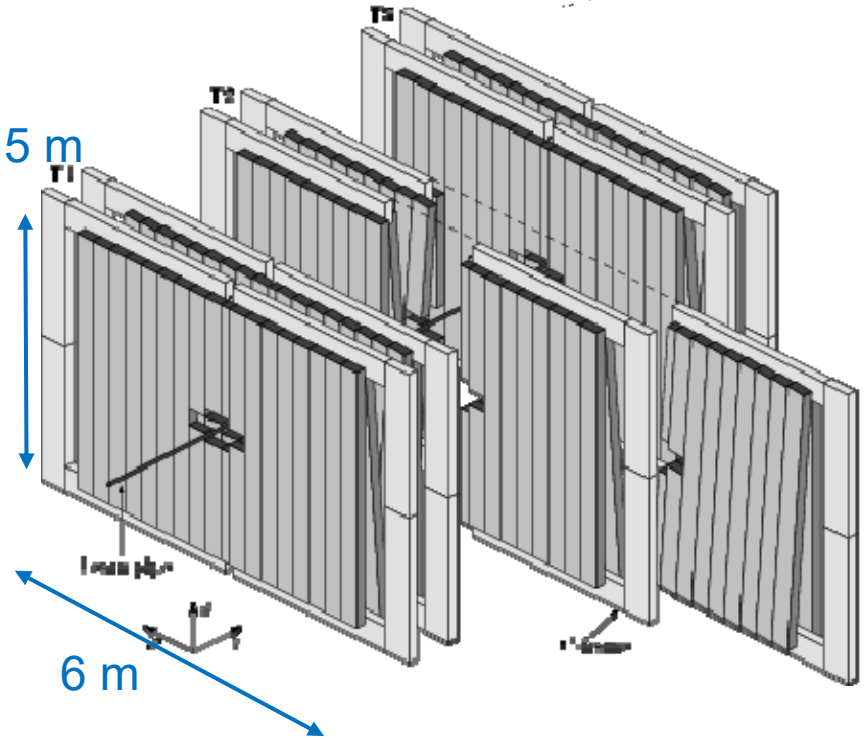

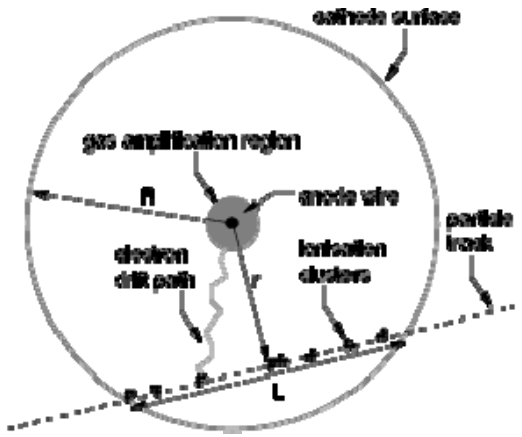

170 μm resolution over
360 m^2 detection areas

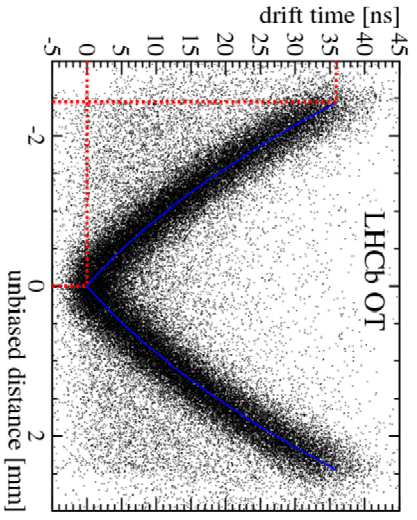

Drift time space relation

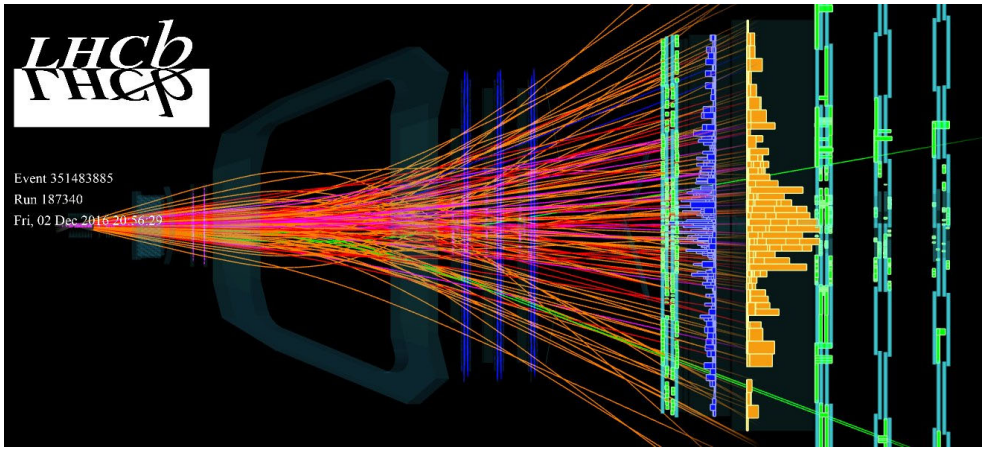

Semiconductor strip & pixel detectors

Semiconductor detectors based on depleted np-junctions (diodes)

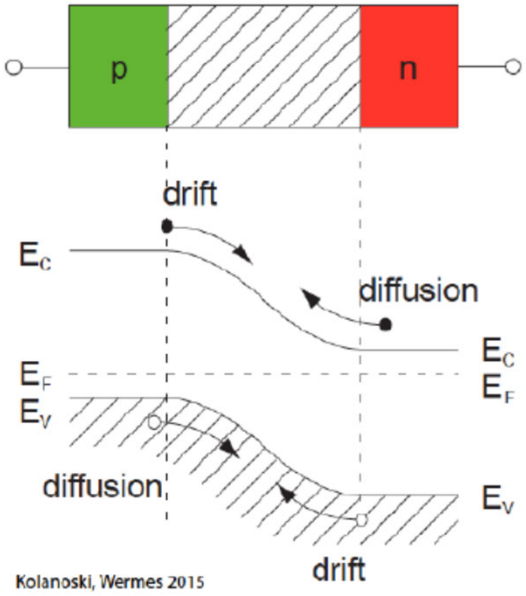

In the junction of p(n) doped semicondutors, the majority charge carriers will diffuse into the other region until the Fermi level is equalized.

Around the junction, there is a region w/o free charge carriers: depletion zone. A space charge is created (pos / neg on n / p-side).
The related electrical field produces a drift of charge carriers which compensates the diffusion.

The depletion zone can be enlarged by applying an external voltage.

With p-doping larger than n-doping, the depletion zone extends mostly into n.

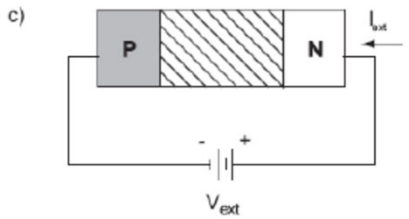

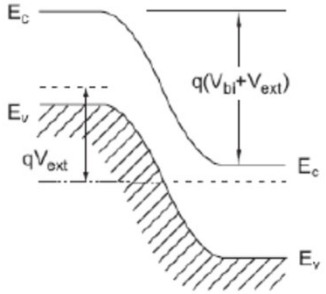

"reverse biasing"

Size of depletion zone:

$$d \approx x_n \approx \sqrt{\frac{2\epsilon\epsilon_0}{e}\frac{1}{N_D}(U_{bin}+U_{ext})}$$

$$\approx 3.6 \cdot 10^3 \sqrt{\frac{U_{ext}}{N_D(\mathrm{V\,cm})}}$$

~300 μm reachable

N_D = doping concentration

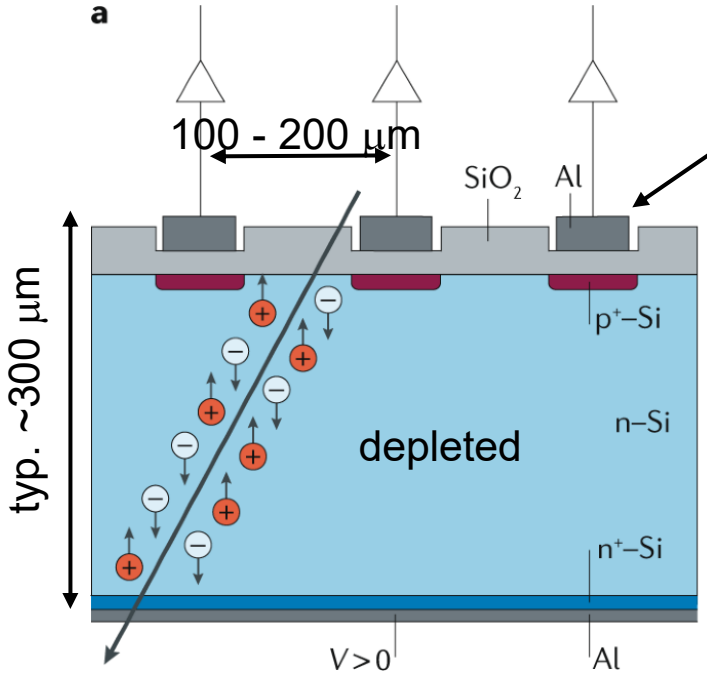

typ. strip length (into the figure plane) is O(10cm)

Typ: N_D (n) = O(10^{12}) N_A (p+) = 10^{16} - 10^{19}

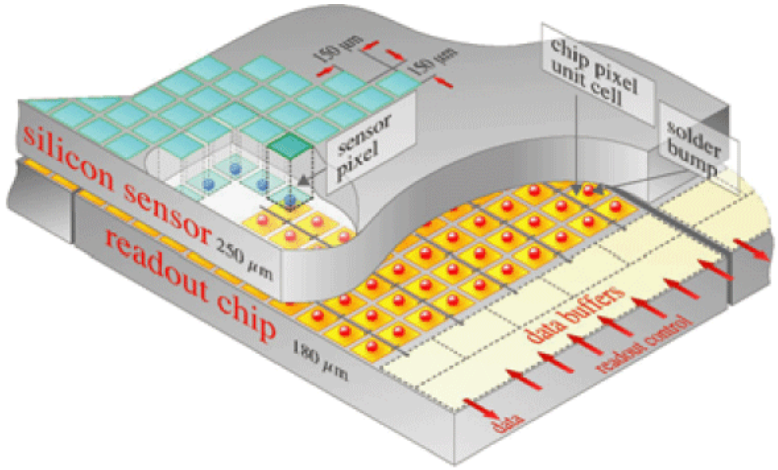

Schematics of a silicon strip sensor:

Strongly doped p^+-strips w/ aluminum contacts on weakly doped n-bulk which has an aluminum contact (by technical reasons there is a thin layer of strongly doped n-Si in between). Charge carriers (electrons) created by particles drift in the applied field to the p+ strips where they are detected.

Schematics of a pixel sensor:

Instead of strips one uses small pixels typ. size 50 x 200…400 μm^2.

Challenge: Readout of the individual channels (please don't conclude from your phone camera – these devices are really very slow) . Requires a readout chip bonded to the pixel matrix: Hybrid pixel detectors.

Novel development: Monolithic pixel sensors with part of electronics in pixel matrix.

(→Heidelberg: Mu3ePix and MightyPix).

Example 1: CMS Tracker

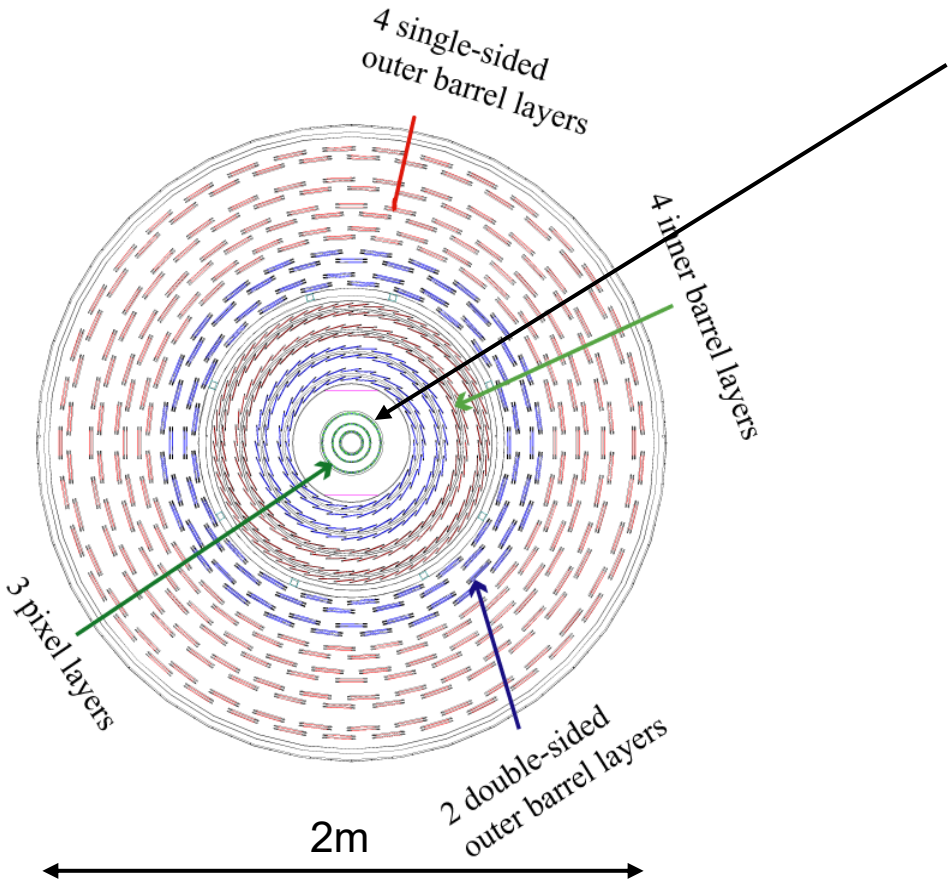

Silicon Pixel detector:
about 66 million 100×150 μm^2 pixels arranged at distance of 4 to 11 cm

Silicon strip detectors:
divided in the inner barrel part (TIB), the inner disks (TID), the outer barrel (TOB) and outer end-caps (TEC).

Tracker contains 15,200 sensitive modules with a total of about 10 million detector strips.

Strip distance = 80 μm to 200 μm
w/ strip widths about 25%

Spatial resolution: 20 – 30 μm

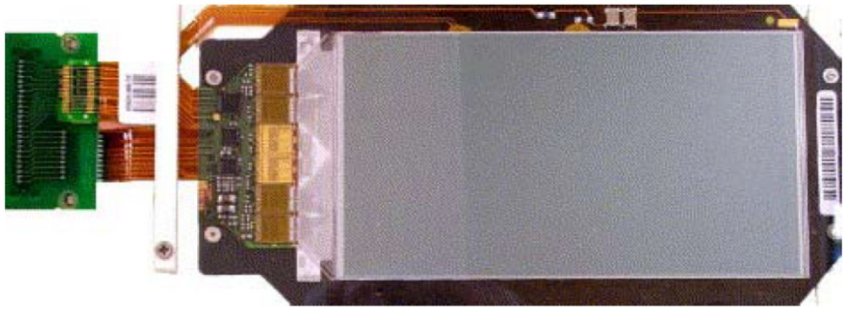

CMS TIB silicon strip modules.

Example 2: ATLAS Inner Tracker

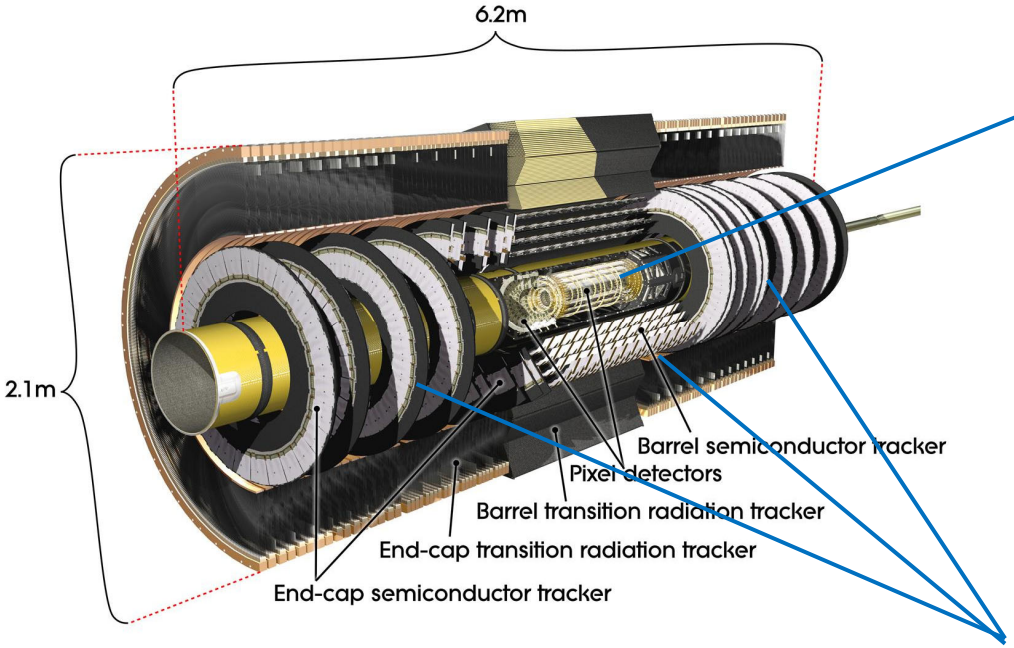

ATLAS pixel detector:

- 92 million pixels (92 million electronic channels).
- Silicon area approx. 1.9m^2
- Pixel 50 x 400μm^2 and 50 x 250 μm^2 for outer / inner external
- 4-barrel layers with 1736 modules
- 3 disks per end-cap w/ 288 modules
- Typ. Spatial resolution: 10 μm

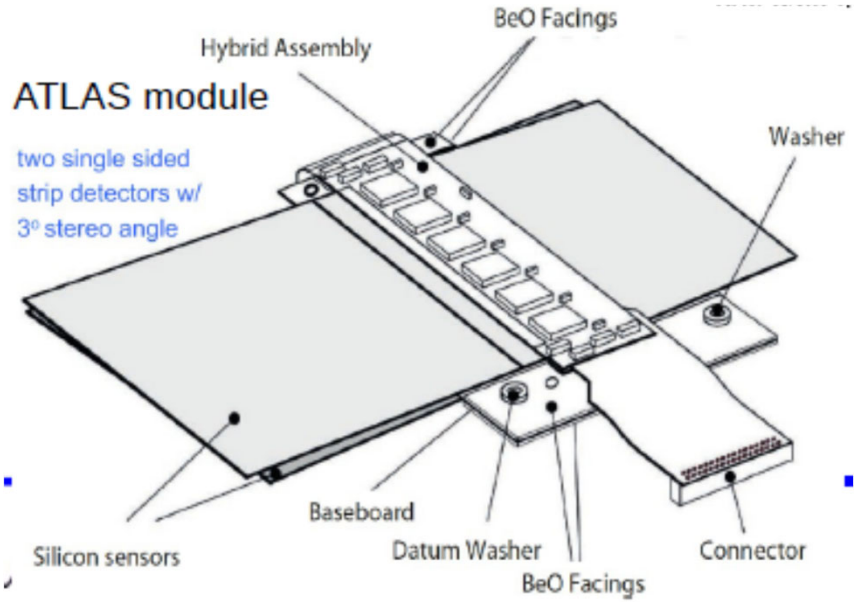

ATLAS strip detector:

4,088 two-sided modules and over 6 million implanted readout strips (6 million channels) 60m^2 of silicon distributed over 4 cylindrical barrel layers and 18 planar endcap discs Readout strips every 80μm.

Typ. spatial resolution: 25 μm

Momentum measurement and B field configurations

B-field (perpendicular to measurement plane)

Solenoid:

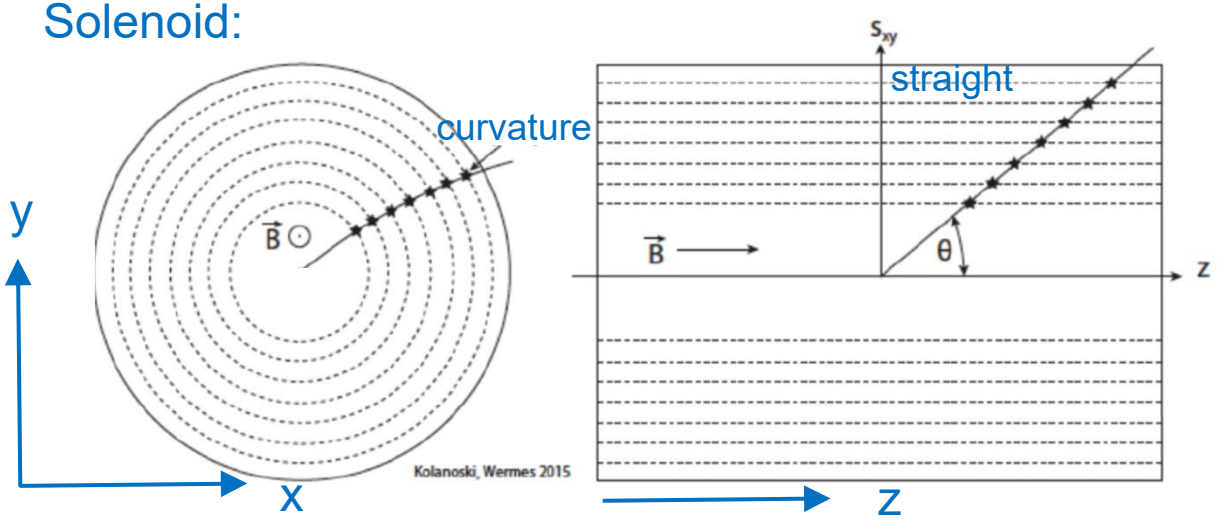

Lorentz force:

$$\vec{F}_{Lorentz} = q\left(\vec{v} \times \vec{B}\right)$$

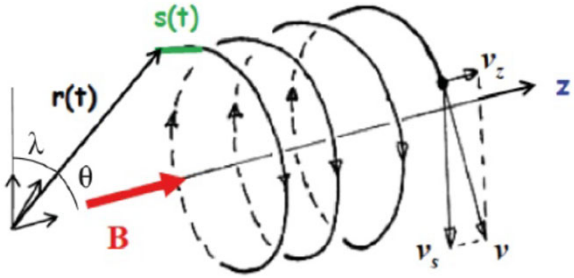

Particle moves on a helical trajectory

Curvature 1/R in xy-plane → particles transverse momentum p_T (within xy plane):

$$p_\perp = q \cdot B \cdot R \quad \text{or} \quad p_\perp[\mathrm{GeV}] = 0.3 \cdot B[\mathrm{T}] \cdot R[\mathrm{m}]$$

The total momentum of the particle is obtained from p = p_T / cos θ

.How well can the transverse momentum be measured? What is its error?

Forward spectrometer configuration (fixed target exp. or forward experiments e.g. LHCb)

Dipole:

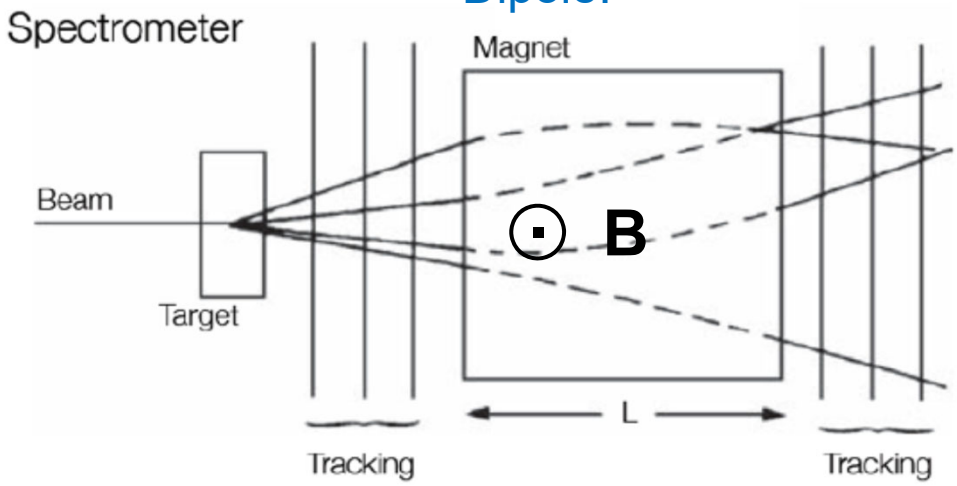

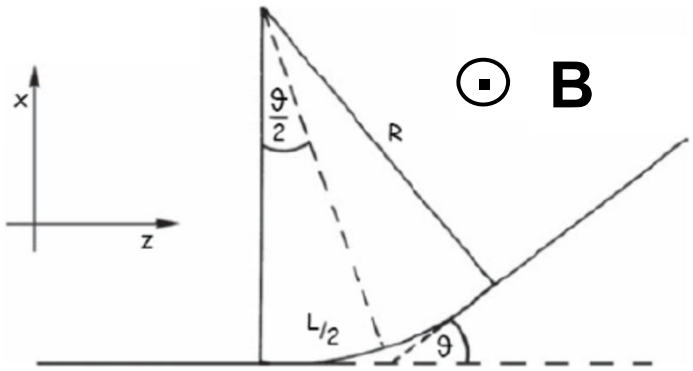

Minimum spectrometer configuration: 2 tracking station before and after magnet
3rd station is used for redundancy, fake rejection

Deflection angle ($p_T \perp B$)

$$\theta \approx \frac{L}{R} = \frac{L}{p_T}\, eB \quad \rightarrow p_T = \frac{eBL}{\theta} = \frac{0.3B[\mathrm{T}]L[\mathrm{m}]}{\theta}$$

$$\rightarrow dp_T = \frac{eLB}{\theta^2} d\theta = \frac{p_T}{\theta} d\theta \quad \rightarrow \frac{dp_T}{p_T} = \frac{d\theta}{\theta}$$

Relative momentum resolution is given by relative angular resolution (depends on spatial resolution of tracker)

Deflection results into momentum-kick Δp_x :

$\Delta p_x = p_T \sin\theta \approx p_T\, \theta = eBL$ often called bending power (spectrometer characteristics)

Assume the minimum tracker configuration w/ 2 + 2 tracking stations w/ spatial resolution σ_x

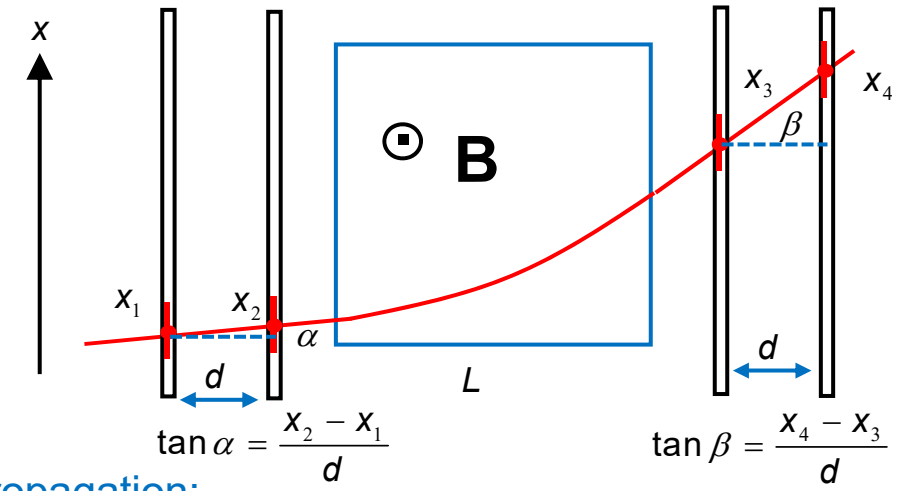

deflection $\theta = \beta - \alpha \approx \tan\beta - \tan\alpha$

$$\theta \approx \frac{x_4 - x_3}{d} - \frac{x_2 - x_1}{d}$$

W/ σ_x same for all layers, one obtains w/ error propagation:

$$d\theta = \frac{2\sigma_x}{d} \quad \text{and with} \quad \frac{dp_T}{p_T} = \frac{d\theta}{\theta}$$

$$\frac{dp_T}{p_T} = \frac{p_T}{eBL}\frac{2\sigma_x}{d} = \frac{p_T}{0.3B[T]L[m]}\frac{2\sigma_x}{d}$$

with $p_T\,\theta = eBL$

For N points before and after magnet: $d\theta = \frac{\sigma_x}{d}\sqrt{\frac{24(N-1)}{N(N+1)}}$

Relative momentum resolution depends on p. Improves for larger field B and larger measurement "arm" L.

There is also a uncertainty on θ from multiple scattering inside the plane:

$$\sigma_{p,MS} = p\sin\theta_{0,MS} \approx p\theta_{0,MS} = p\cdot\frac{13.6\text{MeV}}{\beta p}\sqrt{\frac{L'}{X_0}} = 13.6\text{MeV}\sqrt{\sum\frac{\ell_i}{X_{0,i}}}$$

Should consider sum of all materials

Contribution to p_T resolution results from the comparison w/ p-kick and bending power:

$$\frac{\sigma_{p_T,MS}}{p_T} = \frac{\sigma_{p_T,MS}}{\Delta p_x}_{\text{p-kick}} = \frac{13.6\text{MeV}}{eBL}\sqrt{\frac{L'}{X_0}}$$

Contribution from multiple scattering to relative resolution has no momentum dependence (spectrometer property: bending power & material)

Momentum resolution considering detector spatial resolution and multiple scattering is given by:

$$\left.\frac{\sigma_{p_T}}{p_T}\right|_{tot} = \sqrt{\left(\left.\frac{\sigma_{p_T}}{p_T}\right|_{det}\right)^2 + \left(\left.\frac{\sigma_{p_T}}{p_T}\right|_{MS}\right)^2}$$

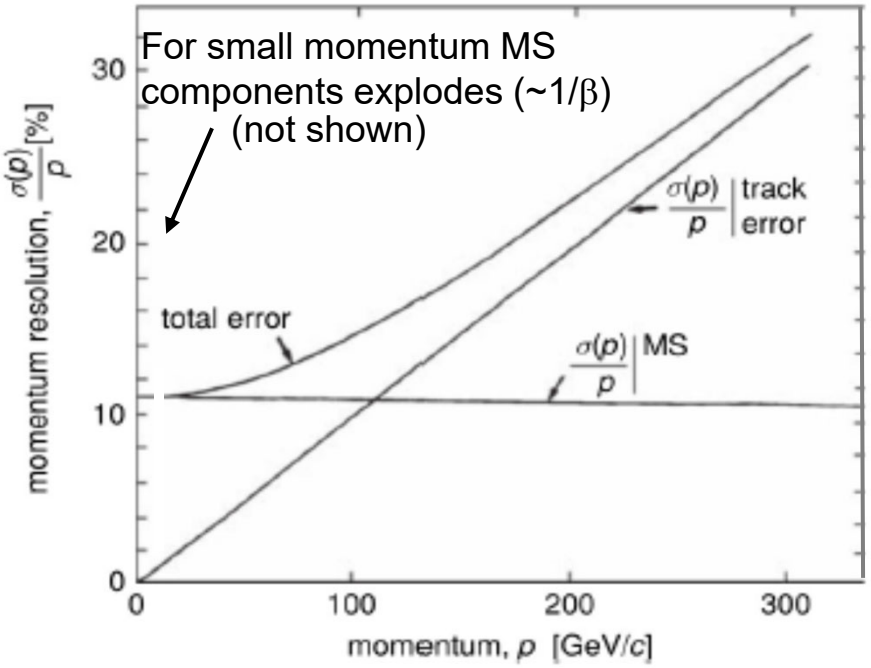

This formula can be applied to more complicated cases – e.g. measurement of the track curvature be cylindrical tracking detector. Assuming the curvature is measured by N space points over distance L one finds for the detector resolution:

$$\left.\frac{\sigma_{p_T}}{p_T}\right|_{det} = \frac{p_T}{0.3\,BL^2}\frac{\sigma_{Hit}}{}\sqrt{\frac{720}{N+4}} \quad \text{for } N \geq 10$$

(B in T, L in m, p in GeV)

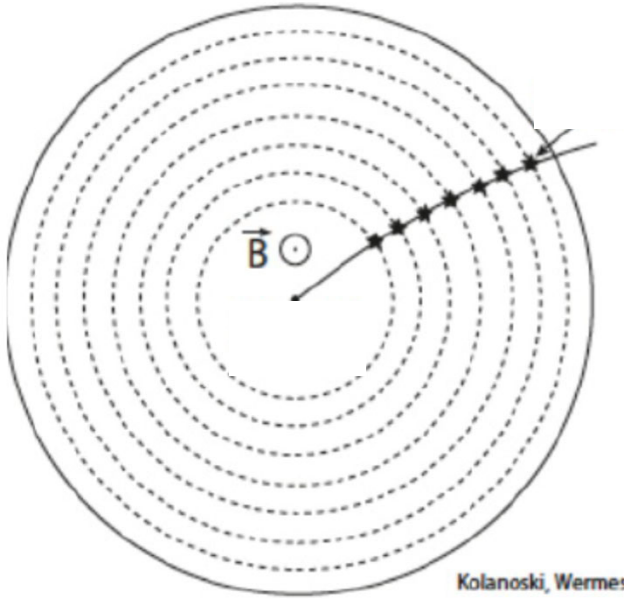

(In literature referred as Gluckstern formula)

Track reconstruction:

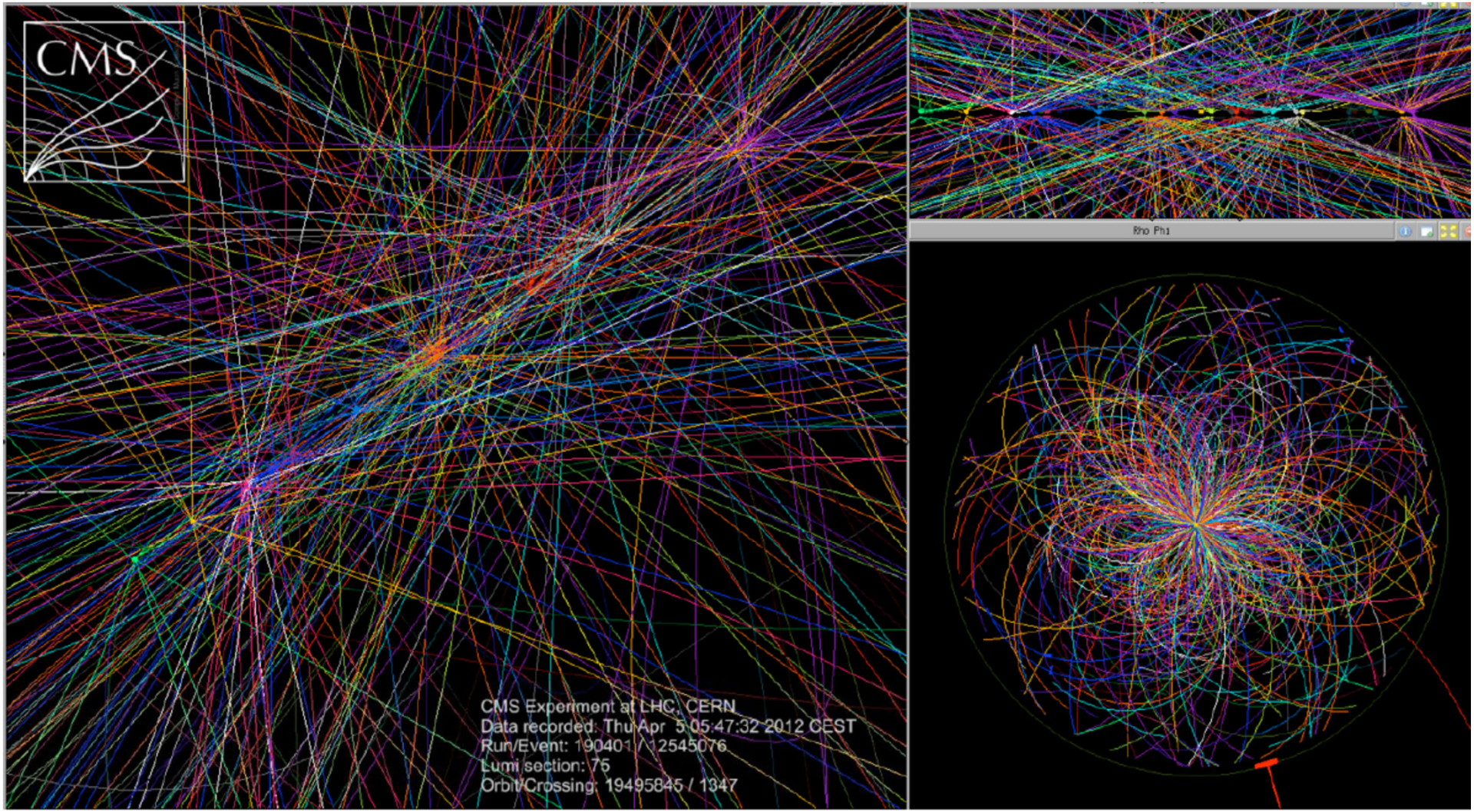

Track reconstruction:

Track reconstruction is usually split into two separate steps:

- **Pattern recognition**: detector hits (space points) are assigned to individual tracks
- **Fit of track model** to space points, accounting for resolution & multiple scattering

Pattern recognition: here w/ local tracklets

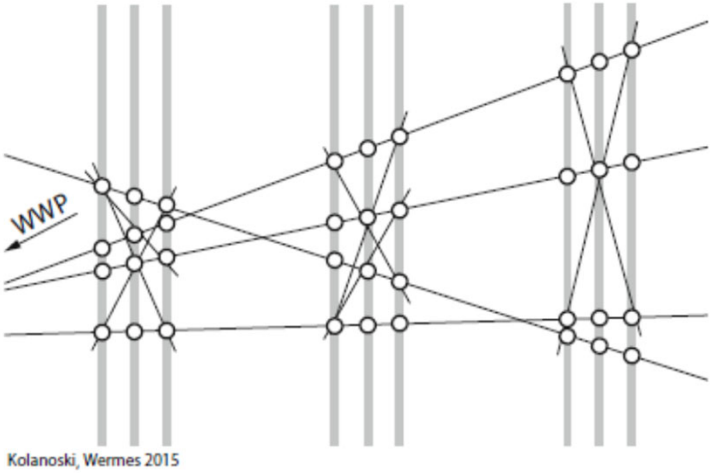

Find locally all possible combinations (tracklets)

Combine local stubs to global tracks

Fit the hits of tracks by a track model.
Often: Kalman filter fit to consider scattering and refine track model.

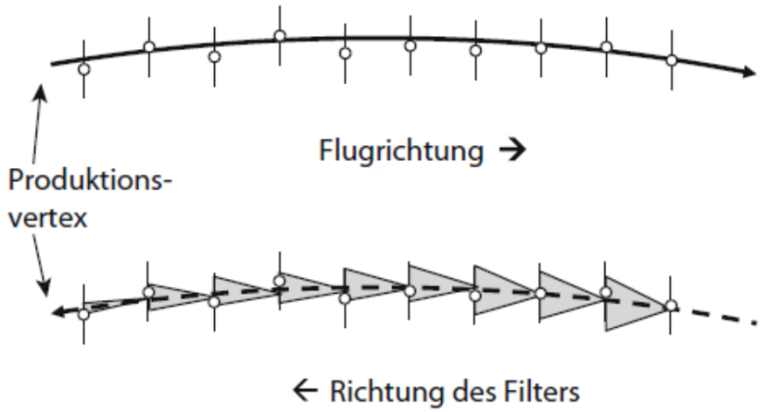

In this way the track model at the last point (close to vertex) is optimized and allows best prediction of vertex.

Tracking detector layout optimized to allow fast and efficient pattern recognition and very good prediction of the vertex from the fitted track model at the last hit.